



## Abstract

43  
44  
45  
46  
47  
48  
49  
50  
51  
52  
53  
54  
55  
56  
57  
58  
59  
60  
61  
62  
63  
64  
65  
66  
67  
68  
69  
70  
71  
72  
73  
74  
75  
76  
77  
78  
79  
80

### Background

Transposable elements (TE) are an important source of evolutionary novelty in gene regulation. However, the mechanisms by which TEs contribute to gene expression are largely uncharacterized.

### Results

Here, we leverage Roadmap and GTEx data to investigate the association of TEs with active and repressed chromatin in 24 tissues. We find 112 human TE types enriched in active regions of the genome across tissues. SINEs and DNA transposons are the most frequently enriched classes, while LTRs are often enriched in a tissue-specific manner. We report across-tissue variability in TE enrichment in active regions. Genes with consistent expression across tissues are less likely to be associated with TE insertions. TE presence in repressed regions similarly follows tissue-specific patterns. Moreover, different TE classes correlate with different repressive marks: Long Terminal Repeat Retrotransposons (LTRs) and Long Interspersed Nuclear Elements (LINEs) are overrepresented in regions marked by H3K9me3, while the other TEs are more likely to overlap regions with H3K27me3. Young TEs are typically enriched in repressed regions and depleted in active regions. We detect multiple instances of TEs that are enriched in tissue-specific active regulatory regions. Such TEs contain binding sites for transcription factors that are master regulators for the given tissue. These TEs are enriched in intronic enhancers, and their tissue-specific enrichment correlates with tissue-specific variations in the expression of the nearest genes.

### Conclusions

We provide an integrated overview of the contribution of TEs to human gene regulation. Expanding previous analyses, we demonstrate that TEs can potentially contribute to the turnover of regulatory sequences in a tissue-specific fashion.

**Keywords:** Transposons, gene regulation, tissue-specific, transcription factors

## 81 **Background**

82 Sequences derived from transposable element (TE) insertions make up roughly half  
83 of the length of the human genome. Several TE groups still show transposing  
84 activity in humans, including Long Terminal Repeat Retrotransposons (mostly ERV1-  
85 LTRs; [1–3]), Long Interspersed Nuclear Elements (LINEs, mostly L1s; [4–5]), Short  
86 Interspersed Nuclear Elements (SINEs) of the Alu families [6,7], and SINE-VNTR-  
87 *Alus* (SVAs; [8,9]).

88 Multiple elegant studies have demonstrated that TE sequences play a functional role  
89 in eukaryotic gene regulation [10–32]. Consistently, we recently demonstrated that  
90 TEs are the primary source of evolutionary novelty in primate gene regulation, and  
91 reported that the large majority of newly evolved human and ape specific liver cis-  
92 regulatory elements are derived from TE insertions [33]. Similarly, other studies  
93 have shown that the recruitment of novel regulatory networks in the uterus was likely  
94 mediated by ancient mammalian TEs [21,22], and that TEs have a role in  
95 pluripotency [34]. Conversely, other researchers have proposed that TE exaptation  
96 into regulatory regions is rare [35], and that TE silencing may not be a major driver of  
97 regulatory evolution in primates [36].

98 Given these contrasting lines of evidence, we aimed to shed light on the contribution  
99 of TEs to the evolution of the tissue-specific regulation of human gene expression.  
100 For this purpose, we took advantage of publicly available data [37,38] to investigate  
101 patterns of TE overlap with tissue-specific histone modification states and to  
102 characterize the contribution of TEs to tissue-specific gene expression. We find that  
103 a significant fraction of the existing human TEs are enriched in regions of the  
104 genome bearing epigenetic hallmarks of active or repressed chromatin, suggesting  
105 they could potentially be actively regulated by the cellular machinery. DNA

106 transposons and SINEs represent the most frequently enriched classes across  
107 tissues, while LTR-ERV1s are the TEs that more commonly show tissue-specific  
108 enrichment and active regulatory activity. TE enrichment in active and repressed  
109 chromatin exhibits tissue-specific patterns. Genes with consistent expression across  
110 tissues are less likely to be associated with a local TE insertion. We detect multiple  
111 instances of TEs showing tissue-specific enrichment in active and repressed regions,  
112 and demonstrate that they contain binding sites for transcription factors that are  
113 tissue-specific master regulators.

114

## 115 **Results**

### 116 **Specific TE families are enriched in active and repressed genomic regions**

117 To investigate the extent to which TEs contribute to the regulation of human  
118 gene expression, we leveraged publicly available data from the Roadmap  
119 Epigenomics Project [37] and from the GTEx Project [38]. We focused on 24  
120 primary tissues and cell types that were processed by both consortia  
121 (Supplementary Table S1). Using five different histone modifications (H3K4me1,  
122 H3K4me3, H3K36me3, H3K9me3, and H3K27me3), Roadmap segmented the  
123 human genome into 15 regulatory classes, reflecting different degrees and types of  
124 regulatory activity. We took advantage of this classification to define active  
125 (H3K4me1, H3K4me3, H3K36me3) and repressed (H3K9me3, and H3K27me3)  
126 chromatin regions in each of the studied tissues.

127 To test for TE enrichment in active and repressed chromatin, we used the TE-  
128 Analysis pipeline ([39]; <https://github.com/4ureliek/TEanalysis>; Supplemental File  
129 S1). This pipeline is designed to output the TE composition of given features, such  
130 as TE counts and TE amounts, aiming to detect potential TE enrichments in the

131 select features. As expected, we find that the majority of human TEs are significantly  
132 depleted from regions marked as active by Roadmap histone modifications (mean  
133 83.9% of TEs; FDR <5%; Supplementary Table S2). Nevertheless, 112 TE families  
134 (9.07% of the annotated TE families in the human genome) are significantly enriched  
135 in active chromatin in at least one tissue (FDR <5%; Fig. 1a; Supplementary Table  
136 S2). These data suggest variability across tissues: aorta, brain anterior caudate, and  
137 adipose are the most “permissive” tissues, while right atrium and spleen do not show  
138 any significant TE enrichment in active regions (Fig. 1a).

139 SINEs and “cut and paste” DNA transposons are the classes most frequently  
140 enriched in active chromatin (Fig. 1b). SINE families, the most abundant human TEs  
141 (38.8% of the total), correspond to 43–66% of the TEs enriched in active regions  
142 (FDR < 5%), these fractions being more than expected by chance in all tissues  
143 (Proportion Test  $p < 2.2 \times 10^{-16}$  for each tested tissue). Similarly, DNA TEs, that  
144 account for 11.3% of the annotated TEs, represent 29–47% of the transposons  
145 enriched in active regions (Proportion Test  $p < 2.2 \times 10^{-16}$  for each tested tissue). In  
146 general, SINE-Alu elements are the most commonly enriched TEs (Supplementary  
147 Table S2).

148 Conversely, LTRs and LINEs are significantly depleted from active genomic  
149 regions of all tissues (Proportion Test  $p < 2.2 \times 10^{-16}$  for each tested tissue; Fig. 1b).  
150 Finally, SINE-VNTR-*Alus* (SVAs), which are the least abundant TEs in the human  
151 genome (0.12% of the total annotated TEs in the human genome), are significantly  
152 overrepresented in active chromatin in 13/24 tissues; Fig. 1b).

153 We set out to investigate the TEs overlapping active regions. These TEs are  
154 depleted in active promoters and intergenic regions, but significantly enriched within  
155 active regions inside gene bodies, and in particular in introns (Fisher’s Exact Test  $p$ -

156 *values* in Fig. 1c). More specifically, 96.3% of TEs enriched in gene bodies overlap  
157 introns, in line with the normally observed distribution of introns and exons in the  
158 human genome (Fig. 1c, Fisher's Exact Test  $p > 0.05$ ). We speculate that genomic  
159 regions containing active genes are more frequently accessible, thus providing a  
160 substrate for TEs to insert. Moreover, TEs present in the bodies of active genes may  
161 be less likely to be silenced than TEs in intergenic regions.

162         Using the same approach previously described for the active regions, we  
163 searched for TEs enriched in repressed genomic regions. Overall, 314 human TE  
164 families (25.4%) are significantly enriched in repressed regions of the genome in at  
165 least one tissue (FDR <5%; Fig. 2a; Supplementary Table S3). LTRs (predominantly  
166 ERV1) represent the large majority of the repressed TEs (Fig. 2b), followed by LINEs  
167 (predominantly L1s) and DNA TEs. Notably, ERV LTRs and L1 LINEs are among  
168 the most active TEs in the genome, and also have their own regulatory architecture  
169 [40, 41]. We thus surmise that these autonomous active TEs may be preferential  
170 targets of repressive marks.

171         We note a very high variability in the number TE families enriched in  
172 repressed regions across tissues (Fig. 2a), as well as large differences in the  
173 composition of enriched TE classes in the repressed regions. Notably, the tissues  
174 that harbor the highest number of TE families enriched in repressed regions  
175 (pancreas, aorta, lung, spleen, esophagus, breast, and liver; Fig. 2a) are also those  
176 displaying the highest numbers of enriched LINEs in the same repressed regions  
177 (Fig. 2b).

178

179 **Different TE repression patterns in the human genome**

180 We examined whether TEs preferentially overlap regions repressed via  
181 Polycomb Repressive Complex (H3K27me3) or via Heterochromatin (H3K9me3).  
182 Overall, 78.6% of the regions classified as repressed in the human genome across  
183 all tissues are bound by H3K27me3 (Polycomb Repressive Complex), while 21.4%  
184 are marked by H3K9me3 (Heterochromatin conformation). However, when we  
185 restrict the analysis to the repressed regions containing a TE, we report an overall  
186 higher than expected overlap with H3K27me3 (median across tissues 85.5%;  
187 Proportion Test across tissues  $p < 2.2 \times 10^{-16}$ ; Supplementary Table S4; Fig. 2C),  
188 and a consequent underrepresentation of H3K9me3 (median 15.5%; Supplementary  
189 Table S4; Proportion Test  $p < 2.2 \times 10^{-16}$ ; Fig. 2d). In 20/24 of the tested tissues,  
190 TEs are marked by H3K27me3 more than expected by chance (Proportion Test  $p <$   
191  $2.2 \times 10^{-16}$  for each of the 20 significant tissues; Supplementary Table S4). In the  
192 remaining four tissues this histone mark is instead underrepresented, while  
193 H3K9me3 is overrepresented: breast (H3K27me3 = 76.4%; Supplementary Table  
194 S4; Proportion Test  $p < 2.2 \times 10^{-16}$ ), aorta (55.1%; Supplementary Table S3;  $p < 2.2$   
195  $\times 10^{-16}$ ), lung (48.9%; Supplementary Table S4;  $p < 2.2 \times 10^{-16}$ ), and spleen (26.5%;  
196 Supplementary Table S3;  $p < 2.2 \times 10^{-16}$ ). Notably, in these four tissues we detect  
197 the highest numbers of TE families enriched in repressed regions (Fig. 2a), and the  
198 highest proportion of repressed LINEs. We speculate that the heterochromatin state  
199 (H3K9me3) may be employed to target specific TE classes and families in a context  
200 specific manner [36].

201 We therefore tested whether different TE classes correlate with either  
202 heterochromatin (H3K9me3) or with Polycomb repressed chromatin (H3K27me3).  
203 LTRs, LINEs, and SVAs are overrepresented in regions marked by H3K9me3  
204 (Fisher's Exact Test  $p < 2.2 \times 10^{-16}$ ; Fig. 2d). Conversely, SINEs and DNA TEs are

205 significantly more likely to overlap H3K27me3 than expected by chance (Fisher's  
206 Exact Test  $p < 2.2 \times 10^{-16}$ ; Fig. 2d). Notably, SVAs are depleted from the regions  
207 marked by H3K27me3 (Fig. 2d).

208 These findings are consistent with recent reports suggesting that H3K27me3 and  
209 H3K9me3 target different transposon types in embryonic stem cells [42], and with a  
210 study reporting that LINEs, LTRs, and SVAs are the most abundant TEs repressed  
211 by H3K9me3 in induced pluripotent stem cells [42].

212

### 213 **Ancient TEs are enriched in active regions, while young TEs are repressed**

214 We clustered the annotated human TEs in 35 age classes as in ref. 39 (e.g.  
215 Eutheria, Primates, Hominidae; Supplemental Table S6), and used the TE-Analysis  
216 shuffling script to test for enrichment of each age class in a given set of regions (see  
217 Methods). Using this approach, we assessed the age of TEs enriched in active and  
218 repressed genomic regions. Ancient TE classes (i.e. age classes older than the  
219 Eutheria lineage) are enriched in the active regions of all tested tissues (FDR <5%;  
220 Supplemental Table S6). These TEs are largely vertebrate or mammalian specific  
221 (Supplemental Table S6). Notably, the only tissues with an enrichment of young TEs  
222 (specifically primate specific) are blood related (Mononuclear and Lymphoblastoid  
223 Cells). These results are in agreement with an elegant study that discovered a key  
224 role of primate specific TEs in the regulatory evolution of immune response [25]. TE  
225 families enriched in active regions across at least 20 of the 24 tissues correspond to  
226 DNA TEs and SINEs (Supplemental Table S2). Despite a lack of enrichment of all  
227 young TEs taken together in active regions, 24 *Alu* families are in fact enriched in  
228 active regions.



229 In contrast, young TEs (i.e. TE classes younger than the Eutheria lineage  
230 split) are significantly enriched in the repressed regions of most tissues. In particular  
231 human specific TEs are enriched in the repressed regions of all brain related tissues  
232 (FDR <5%; Supplemental Table S6). These young TEs correspond to ERV LTRs, L1  
233 LINEs, and SVAs, but only one family is found enriched in at least 20 tissues  
234 (MER52A), which is in line with the broad cross-tissue variability of the TEs enriched  
235 in repressed chromatin regions (see above).

236 Collectively, these data suggest that young TEs are predominantly silenced, while  
237 the older TE fragments still detectable in the human genome are now more tolerated.

238

### 239 **TE insertions are associated with gene expression variance across tissues**

240 We employed GTEx data to test if TE insertions affect local gene expression.  
241 For this purpose, we first assigned each TE overlapping an active genomic region to  
242 its nearest gene transcription start site (TSS). Next, we divided all human genes in  
243 four categories (Supplemental Table S7): 1) Genes associated with TEs that are only  
244 found in active regions across tissues; 2) Genes associated with TEs that are found  
245 in active or repressed regions in a tissue-specific fashion; 3) Genes associated with  
246 TEs that are only found in repressed regions; 4) Genes never associated with TE  
247 insertions. Based on this classification, genes associated with a TE insertion in  
248 regions that are active in at least one tissue are characterized by significantly higher  
249 expression variance (normalized by mean expression) than genes either associated  
250 to repressed TEs or not associated to a TE (Wilcoxon's Rank Sum Test  $p < 2.2 \times 10^{-16}$ ;  
251 Fig. 3). Similarly, the genes associated with TEs exclusively found in active  
252 regions have significantly higher expression variance than the genes associated with  
253 TEs present in both active and repressed regions (Wilcoxon's Rank Sum Test  $p =$

254  $9.91 \times 10^{-8}$ ; Fig. 3). We reasoned that TE insertions may happen more likely at  
255 longer genes located in gene deserts. However, even after correcting our model for  
256 gene density and gene length, the gene expression variance is still positively  
257 correlated with TE insertion in active regions (linear regression  $p < 2.2 \times 10^{-16}$ ).

258 Together, these findings suggest that genes with local TEs overlapping active  
259 chromatin have higher variability in gene expression across tissues, and that genes  
260 consistently expressed across tissues (e.g. housekeeping and other essential genes)  
261 may be less tolerant towards TE insertions in their regulatory regions.

262

### 263 **Tissue-specific TE enrichment in active regions correlates with tissue-specific** 264 **gene expression**

265 We compared the relative enrichment in active regions of each TE family  
266 across tissues. Specifically, for each TE enriched in active regions (FDR < 5%), we  
267 leveraged the Odd Ratios from the permutation test of the TE-Analysis pipeline to  
268 compute Z-scores (i.e. effect sizes; see methods), and compare them across  
269 tissues. We find that TE enrichment varies substantially across tissues  
270 (Supplemental Table S5; Fig. 4), and many TEs exhibit tissue-specific enrichment in  
271 active chromatin (Fig. 4). For example, HERV15 (LTR) is significantly more enriched  
272 in the liver and in the stomach mucosa compared to any other tissue (Fig. 4). Motif  
273 analysis revealed that the liver regions of active histone modification overlapping  
274 HERV15 are enriched in motifs for EOMES (Supplemental File S2). This  
275 transcription factor (TF) has a key role in the hepatic immune response, instructing  
276 the development of two distinct natural killer cell lineages specific to this tissue [43].  
277 Moreover, EOMES is also an established tumor suppressor in Hepatocellular  
278 Carcinoma [44]. Notably, HERV15 was recovered as significantly enriched in the

279 human liver enhancers also in our previous study [33], suggesting that the findings of  
280 the present analysis are not likely to represent batch-specific effects of the Roadmap  
281 data.

282 Similarly, X7C (LINE) and Charlie15a (DNA TE), are the most enriched TEs  
283 within regions bearing active chromatin state in the breast. In the sequence of these  
284 we find enrichment for binding sites for key breast TFs as KLF5 and CPEB1 (Fig. 5a;  
285 Supplemental File S2). Notably, KLF5 is an essential regulator of hormonal  
286 signaling and breast cancer development [45], and is considered a breast cancer  
287 suppressor [46]. Similarly, CPEB1 mediates epithelial-to-mesenchyme transition in  
288 breast, and mice depleted of this gene showed increased breast cancer metastatic  
289 potential [47]. Interestingly Charlie15a shows tissues-specific depletion in the  
290 mononuclear blood cells (Fig. 4), highlighting a potential tissue-specific regulatory  
291 activity.

292 To assess the robustness of the enrichment of X7C and Charlie15a in the breast, we  
293 ran the TE-Analysis pipeline on publicly available H3K27ac and H3K4me1 data  
294 generated by Encode from the breast epithelium and from the MCF7 cell line [48].  
295 Notably, these two TEs were also significantly enriched in the Encode data (FDR <  
296 5%), suggesting that batch effects are unlikely strong drivers of this trend.

297 Analogously, LTR13\_ is the most enriched TE in the active chromatin of  
298 pancreas and Lymphoblastoid Cell Line (LCL). These LTR copies are enriched for  
299 binding sites for SOX9 and PRDM1/Blimp-1 (Fig. 5d; Supplemental File S2). SOX9  
300 is a master regulator of the pancreatic program [49], while PRDM1/Blimp-1 has a  
301 central role in determining and shaping the secretory arm of mature B Lymphocyte  
302 differentiation [50].

303 We next tested whether tissue-specific TE enrichment in active chromatin  
304 (Fig. 4, 5a–f) correlates with tissue-specific-changes in gene expression.  
305 Specifically, we tested the TE families showing the highest degree of tissue-specific  
306 enrichment (Fig. 4: HERV15/liver, LTR13\_/LCL, X7C-Charlie15a/breast). With the  
307 exception of HERV15/liver (Wilcoxon's Rank Sum Test  $p > 0.05$ ), in the other tested  
308 instances (LTR13\_/LCL; X7C-Charlie15a/breast) the tissue-specific enrichment of  
309 the TEs in active chromatin regions is associated with a significant change in the  
310 associated gene expression (Wilcoxon's Rank Sum Test  $p$ -values in Figs. 5b,e).  
311 These findings support a possible regulatory role for the co-opted TEs.

312 To better understand how these tissue-specific TEs may be involved in the  
313 regulation of gene expression, we investigated what typology of genomic region they  
314 overlap (i.e. promoter, intergenic, introns, exons). Both X7C/Charlie15a in breast  
315 and LTR13\_ in LCLs are significantly depleted in promoter and intergenic regions,  
316 but overrepresented in gene bodies (Figs. 5c, f), 97.8% (X7C/Charlie15a) and 96.4%  
317 (LTR13\_) of them respectively found in introns.

318 The Roadmap data did not include H3K27ac profiles for all tissues. Therefore,  
319 to further characterize these intronic regions, we leveraged again the publicly  
320 available H3K27ac and H3K4me1 Encode data for the breast (Breast epithelium and  
321 MCF7 cell line; [48]). These data reveal that 57.0% of the intronic regions containing  
322 X7C or Charlie15a overlap a H3K27ac or H3K4me1 peak, thus suggesting that most  
323 of these regions likely represent breast intronic enhancers. As comparison, only  
324 33.7% of random intronic regions of the same size and number of the ones  
325 overlapping X7C/Charlie15a TEs are overlap a H3K27ac or H3K4me1 peak (Fisher's  
326 Exact Test  $p < 2.2 \times 10^{-16}$ ).

327 Collectively, these findings point towards a model in which specific TE  
328 families, largely belonging to LTR (ERVs) and DNA TE classes, have more  
329 regulatory potential than other transposons. Furthermore, our data expand upon  
330 previous findings suggesting that ERVs that escape repression can have a  
331 significant impact on the host gene regulation [9, 25, 26, 33, 51, 52].

332

### 333 **SVAs exhibit tissue-specific regulatory activity**

334 In our recent work, we demonstrated that a large fraction of human specific  
335 cis-regulatory elements in the liver are SVA transposons, which typically function as  
336 transcriptional repressors, at least in this tissue [33]. SVAs are very young  
337 transposons, being Hominidae (SVA\_A, B, C and D) and human specific (SVA\_E  
338 and F). According to Roadmap data, SVAs are enriched in the active regions of  
339 13/25 tissues (Fig. 1b), and mainly corresponded to SVA\_A copies (Supplementary  
340 Table S4). We first assessed the potential contribution of SVAs to gene regulation of  
341 two of these tissues: the adipose nuclei and the liver.

342 In both tissues, SVAs provide binding sites for key transcription factors (Fig.  
343 5g, j; Supplemental File S2). ZEB1 is the master regulator of adipogenesis [53, 54],  
344 and, based on GTEx data, is ten times more highly expressed in adipose tissue  
345 compared to the liver. Similarly, SOX6 contributes to the developmental origin of  
346 obesity by promoting adipogenesis, and has a key role in adipocyte differentiation  
347 [55]. Consistent with the data reported for other tissues, SVAs associated with  
348 active chromatin in adipose nuclei and liver are strongly enriched in gene bodies  
349 (Figs. 5i, l). Genes associated with SVAs in the adipose nuclei are significantly more  
350 highly expressed in this tissue compared to other tissues (Wilcoxon's Rank Sum

351 Test  $p = 0.0002$ ; Fig. 5h), suggesting that SVA elements can work as transcriptional  
352 activators, at least in the adipose tissue.

353 In the liver, SVAs in active regions are enriched for hepatic regulators like  
354 CPEB1, that mediates insulin signaling in the liver (Fig. 5j; [56]), and STAT3, that  
355 regulates liver regeneration and immune response and negatively modulates insulin  
356 action (Fig. 5j; [57]). However, the liver SVAs are also enriched for established  
357 transcriptional repressors, like Smad3 (Fig. 5j). Consistently, genes associated with  
358 liver active SVAs exhibit lower expression in this tissue compared to all the others  
359 (Wilcoxon's Rank Sum Test  $p < 2.2 \times 10^{-16}$ ; Fig. 5k), supporting the previously  
360 proposed repressive role of SVAs in the hepatic system [33].

361

## 362 **Discussion**

363 The contribution of transposable elements (TEs) to gene regulation was proposed  
364 over half a century ago [10–13] and considerably expanded over the last two  
365 decades, largely due to the advances in next generation sequencing [14–36].

366 In order to gain insights in this topic, we identified TEs enriched in active and  
367 repressed genomic regions of 24 human tissues, using Roadmap and GTEx data.

368 Our analyses provide a novel integrated overview of the potential impact of TEs to  
369 the human gene regulation across multiple tissues, correlating the enrichment of TE  
370 copies in active chromatin to tissue-specific gene expression. In fact, many of the  
371 previous studies have proposed that TEs are frequently enriched in cis-regulatory  
372 elements and lncRNAs [21, 22, 33, 39, 58], but the actual effect of the presence of  
373 TEs on the associated gene expression was not tested on a large scale.

374 Recent work has evaluated the prevalence of TE-derived DNA in enhancers and  
375 promoters across mouse cell lines and primary tissues [35]. The present study builds

376 upon this by investigating the dynamics of TE recruitment and the potential effects  
377 on tissue-specific gene expression.

378 We demonstrate that ~10% of the TEs identified in the human genome are  
379 significantly enriched in active regions (promoters, intergenic enhancers, intronic  
380 enhancers) of 24 different human tissues. In general, we report a high degree of  
381 variability of TE enrichment in the active and repressed genome across tissues, and  
382 detect multiple instances of TEs displaying potential tissue-specific regulatory  
383 function. We acknowledge that the correlation between tissue-specific TE  
384 enrichment in active regions and the tissue-specific changes in gene expression  
385 does not necessarily underly a causal role for the TEs. On the other hand, while it is  
386 possible that the changes in gene expression are simply due to the presence of a  
387 tissue-specific active histone mark, we also find that in all of the tested cases the  
388 enriched TE sequence provides binding sites for transcription factors that are master  
389 regulators for that specific tissue. This is consistent with the changes in the gene  
390 expression of associated (i.e. adjacent) genes and could explain why these TE  
391 insertions are retained by selection.

392 Enriched TEs are typically distributed along gene bodies, likely functioning as  
393 intronic enhancers. We reason that this may be explained by the assumption that  
394 TEs located within intra-genic regions are less likely to be repressed or removed. In  
395 agreement with these findings, a recent study has shown that TEs are depleted in  
396 human promoters and intergenic enhancers across multiple tissues [35]. In this  
397 context, we see a correlation between gene expression variance and the insertion of  
398 TEs in their loci or regulatory regions. This may suggest that genes consistently  
399 expressed across tissues are less prone towards TE co-option in their regulatory

400 networks, but future analyses in this direction will be needed to further characterize  
401 this phenomenon.

402 On the other hand, L1 LINEs and ERV LTRs are the most frequently enriched TE  
403 classes in the repressed regions. L1 retrotransposons are among the most active  
404 TEs in the human genome [59], and several studies have demonstrated that they are  
405 also active in brain tissues (e.g. hippocampus), and can contribute to neuronal  
406 genetic diversity in mammals [60–63]. Both L1s and LTRs possess their own  
407 regulatory architecture, and we speculate that their preferential silencing prevents  
408 these TEs from interfering with gene regulatory networks. Despite this, we  
409 demonstrate that LTRs that escape repression may be co-opted in a tissue-specific  
410 manner in the active regulatory regions, putatively as a consequence of their  
411 regulatory potential.

412 We show that TEs enriched in repressed regions of most tissues are generally  
413 young, while TEs enriched in active regions of most tissues generally predate the  
414 split of eutherian mammals. This is consistent with an accumulation of mutations in  
415 these ancient copies that would have increased the likelihood to generate binding  
416 sites for transcription factors, and thus the probability for the TE to be co-opted in the  
417 regulatory networks. An alternative explanation could be that young TE insertions in  
418 active chromatin regions are more likely to be removed by purifying selection than  
419 the new insertions in repressed regions, since the latter are more likely to have a  
420 neutral impact.

421 Finally, we demonstrate that SVAs, previously characterized as transcriptional  
422 repressors in select cell-types [33, 64], can act as both activators or repressors in a  
423 tissue-specific fashion.

424



## 425 **Conclusions**

426 In summary, we present a comprehensive overview of the contribution of TE  
427 copies to human gene regulation: not only do they provide an important source of  
428 evolutionary novelty for the genome, but they can also function with tissue-specific  
429 patterns, modulating the expression of key genes and pathways.

430

## 431 **Methods**

### 432 **TE-Analysis pipeline**

433 To test for TE enrichment in active and repressed regions, we used the TE-Analysis  
434 pipeline v 4.6 ([39]; <https://github.com/4ureliek/TEanalysis>). This pipeline is  
435 designed to output the TE composition of given features, such as TE counts and TE  
436 amounts, aiming to detect potential TE enrichments in the select features. Roadmap  
437 annotated BED files (i.e. files listing the coordinates of annotated genomic regions)  
438 for each of the 24 tissues were downloaded (  
439 [http://egg2.wustl.edu/roadmap/data/byFileType/chromhmmSegmentations/ChmmMo  
440 dels/coreMarks/jointModel/final/](http://egg2.wustl.edu/roadmap/data/byFileType/chromhmmSegmentations/ChmmModels/coreMarks/jointModel/final/); last access: 10/4/2017). One file per tissue was  
441 downloaded (TISSUE\_ID\_coreMarks\_dense.bed.gz"; Supplementary Table S1).  
442 From each of the 24 BED files, we produced two different files: one for the regions  
443 enriched with epigenomics hallmarks of active chromatin (hereafter "active regions".  
444 Histone marks: H3K4me1, H3K36me3, H3K4me3. Roadmap annotations: "TssA",  
445 "TssAFlnk", "TxFlnk", "Tx", "TxWk", "EnhG", "Enh", "TssBiv", "EnhBiv"), and one  
446 for the regions with signature of repressed chromatin (hereafter: "repressed regions".  
447 Histone marks: H3K27me3, H3K9me3. Roadmap annotations: "Het", "ReprPC",  
448 "ReprPCWk").

449 For each tissue, we tested for TE enrichment in the “active” and “repressed”  
450 BED files using the “TE-analysis\_Shuffle\_bed.pl” script v 4.3. Specifically, this script  
451 assesses which TEs are significantly enriched in a set of features (BED files) by  
452 comparing observed overlaps with the average of  $N$  expected overlaps (here 1000).  
453 These expected overlaps were obtained by shuffling the genomic position of TEs. TE  
454 annotations were downloaded from the University of California Santa Cruz Genome  
455 Browser (RepeatMasker, Hg19 version; [65]).

456 The “TE-analysis\_Shuffle\_bed.pl” script was run with Bedtools v2.27.1 [66] and the  
457 following parameters:

458 -f Roadmap\_BEDFILE (active or repressed)  
459 -q RepeatMasker.out (TE file, hg19)  
460 -n 1000 (number of bootstrap replicates)  
461 -r hg19.chrom.sizes  
462 -g 20141105\_hg38\_TEage\_with-nonTE.txt (distributed with the pipeline)  
463 -s rm (shuffles the TEs within their genomics position)

464  
465 The script performs a two-tailed permutation test to assess the enrichment (or  
466 depletion) of each annotated TE in the given regions (Roadmap regions), thus  
467 assigning a  $p$ -value to each annotated TE. Additionally, we corrected for multiple  
468 testing by applying a False Discovery Rate (FDR; [67]). Only TEs with FDR < 5%  
469 were retained, considered significantly enriched in the given tissue, and used for  
470 downstream analyses.

471

472 **Composition of enriched TEs**

473 To characterize TEs enriched within active and repressed regions of each tissue  
474 (e.g. Figs. 1b, 2b), each TE was assigned to one of the major TE classes: DNA  
475 transposons, LINEs, LTRs, SINEs, SVAs, according to RepeatMasker annotations.  
476 To assess the genomic distribution of the enriched TEs (e.g. Figs. 1c, 2c), we  
477 considered as 1) PROMOTERS: all of the regions found within +/- 1 Kb from an  
478 annotated TSS (Gencode\_v19 comprehensive annotations). 2) GENE BODIES: all  
479 of the regions overlapping an annotated gene but not overlapping the promoter  
480 region. 3) INTERGENIC - all of the regions not overlapping an annotated gene and  
481 distant > 1 Kb from a TSS.

482

### 483 **Correlation between TE insertion and variance in gene expression**

484 We calculated the variance and mean of the TPM (Transcripts Per Million) for each  
485 gene using GTEx data. We assigned each TE overlapping an active or a repressed  
486 region to the closest gene, based on the distance to the nearest transcription start  
487 site. Next, we divided all human genes in four categories: 1) Genes associated with  
488 TEs that are only found in active regions across tissues; 2) Genes associated with  
489 TEs that are found in active or repressed regions in a tissue-specific fashion; 3)  
490 Genes associated with TEs that are only found in repressed regions; 4) Genes never  
491 associated with TE insertions. Gene expression variance, normalized by mean  
492 expression, was compared across the four categories. Gene density and gene length  
493 were used as covariates for the model. Specifically, gene density was calculated as  
494 the amount of exonic sequence present within +/- 100 Kb from each gene. In  
495 summary, the following model was used:

496

497  $\text{lm}(\text{normalized\_variance} \sim \text{CATEGORY} + \text{gene\_length} + \text{gene\_density})$

498

499 Variance was normalized by average expression across tissues.

500

### 501 **Computation of Z-scores for tissue-specificity**

502 For each TE enriched in active regions (FDR < 5%), we used the Odd Ratios (OR)

503 from the permutation test of the TE-Analysis pipeline to compute Z-scores with the

504 following equation:  $(OR - \text{mean}(OR)) / \text{sd}(OR)$ . Z-scores can be found in

505 Supplemental Table S5.

506

### 507 **Motif analyses**

508 Motif analyses were performed using the Meme-Suite [68], and specifically with the

509 Meme-ChIP application. Fasta files of the regions of interest were produced using

510 BEDTools v2.27.1. Shuffled input sequences were used as background. *E-values* <

511 0.001 were used as threshold for significance [68].

512

### 513 **Testing for TE co-option on gene expression**

514 For each human gene and for each tissue, GTEx provides the mean of the TPMs

515 (Transcripts Per Million). To test whether tissue-specific TE enrichment correlates

516 with tissue-specific changes in gene expression, for each gene associated with a TE

517 of interest, we used the mean TPMs to compare the expression of genes in the

518 tissue of enrichment Vs the average of the gene expression of the same genes in all

519 the other considered tissues (i.e. mean of TPMs across all the other tissues).

520

### 521 **Statistical and genomic analyses**

522 All statistical analyses were performed using R v3.4.1 [69]. Figures were made with  
523 the package ggplot2 [70]. BEDTools v2.27.1 was used for all the genomic analyses.

524

## 525 **Acknowledgements**

526 We thank Roadmap and GTEx Consortia for the generation of invaluable data. MT  
527 thanks his current P.I. (Alessandro Gardini, The Wistar Institute) who granted him  
528 time and freedom to work on this project. We also thank the two anonymous  
529 reviewers for their valuable suggestions and insights.

530

## 531 **Authors' contributions**

532 MT and CDB designed the project. MT, AK, and CDB analyzed the data. MT, AK,  
533 and CDB wrote and approved the manuscript.

534

535 **Ethics approval and consent to participate:** N/A

536 **Consent for publication:** N/A

537 **Availability of data and material:** N/A

538 **Competing interests:** The authors declare no competing interests.

539 **Funding:** N/A

540

## 541 **References**

- 542 1. Tonjes RR, et al. HERV-K: the biologically most active human endogenous retrovirus  
543 family. *J Acquir Immune Defic Syndr Hum Retrovirol.* 1996;13(1):261–7.
- 544 2. Medstrand P, Mager DL. Human-specific integrations of the HERV-K endogenous  
545 retrovirus family. *J Virol.* 1998;72:9782–7.

- 546 3. Fuchs NV, Loewer S, Daley GQ, Izsvak Z, Lower J, Lower R. Human endogenous  
547 retrovirus K (HML-2) RNA and protein expression is a marker for human embryonic  
548 and induced pluripotent stem cells. 2013. *Retrovirology*;10:115.
- 549 4. Kazazian HH, Wong C, Youssoufian H, Scott AF, Phillips DG, Antonarakis SE.  
550 Haemophilia A resulting from de novo insertion of L1 sequences represents a novel  
551 mechanism for mutation in man. *Nature*. 1988;332:164–6.
- 552 5. Brouha B, Schustak J, Badge RM, Lutz-Prigge S, Farley AH, Moran JV, Kazazian  
553 HH. Hot L1s account for the bulk of retrotransposition in the human population. *Proc*  
554 *Natl Acad Sci USA*. 2003;100:5280–5.
- 555 6. Batzer MA, Deininger PL. A human-specific subfamily of Alu sequences. *Genomics*.  
556 1991;9:481-7.
- 557 7. Batzer MA, Gudi VA, Mena JC, Foltz DW, Herrera RJ, Deininger PL. Amplification  
558 dynamics of human-specific (HS) Alu family members. *Nucleic Acids Res*.  
559 1991;19:3619–23.
- 560 8. Ostertag EM, Goodier JL, Zhang Y, Kazazian HH. SVA elements are non  
561 autonomous retrotransposons that cause disease in humans. *Am J Hum Genet*.  
562 2003;73:1444–51.
- 563 9. Wang H, Xing J, Grover D, Hedges DJ, Han K, Walker JA, Batzer MA. SVA  
564 elements: a hominid-specific retroposon family. *J Mol Biol*. 2005;354:994–1007.
- 565 10. McClintock B. The origin and behavior of mutable loci in maize. *Proc Natl Acad Sci*  
566 *USA*. 1950;36:344–55.
- 567 11. McClintock B. The significance of responses of the genome to challenge. *Science*.  
568 1984;226:792–801.
- 569 12. Britten RJ, Davidson EH. Gene regulation for higher cells: a theory. *Science*.  
570 1969;165:349–57.
- 571 13. Davidson EH, Britten RJ. Regulation of gene expression: possible role of repetitive  
572 sequences. *Science*. 1979;204:1052–9.
- 573 14. Jordan IK, Rogozin IB, Glazko GV, Koonin EV. Origin of a substantial fraction of  
574 human regulatory sequences from transposable elements. *Trends Genet*. 2003;19:68–  
575 72.
- 576 15. Bejerano G, Lowe CB, Ahituv N, King B, Siepel A, Salama SR, Rubin EM, James  
577 Kent W, Haussler D. A distal enhancer and an ultraconserved exon are derived from a  
578 novel retroposon. *Nature*. 2006;441:87–90.
- 579 16. Wang T, Zeng J, Lowe CB, Sellers RG, Salama SR, Yang M, Burgess SM,  
580 Brachmann RK, Haussler D. Species-specific endogenous retroviruses shape the  
581 transcriptional network of the human tumor suppressor protein p53. *Proc Natl Acad*  
582 *Sci USA*. 2007;104:18613–8.
- 583 17. Bourque G, Leong B, Vega VB, Chen X, Lee YL, Srinivasan KG, Chew J-L, Ruan Y,  
584 Wei C-L, Ng HH, et al. Evolution of the mammalian transcription factor binding  
585 repertoire via transposable elements. *Genome Res*. 2008;18:1752–62.
- 586 18. Sasaki T, Nishihara H, Hirakawa M, Fujimura K, Tanaka M, Kokubo N, Kimura-  
587 Yoshida C, Matsuo I, Sumiyama K, Saitou N, et al. Possible involvement of SINEs in  
588 mammalian-specific brain formation. *Proc Natl Acad Sci USA*. 2008;105: 4220–5.

- 589 19. Markljung E, Jiang L, Jaffe JD, Mikkelsen TS, Wallerman O, Larhammar M, Zhang  
590 X, Wang L, Saenz-Vash V, Gnirke A, et al. ZBED6, a novel transcription factor  
591 derived from a domesticated DNA transposon regulates IGF2 expression and muscle  
592 growth. *PLoS Biol.* 2009;7:e1000256.
- 593 20. Kunarso G, Chia NY, Jeyakani J, Hwang C, Lu X, Chan YS, Ng HH, Bourque G.  
594 Transposable elements have rewired the core regulatory network of human embryonic  
595 stem cells. *Nat Genet.* 2010;42:631–4.
- 596 21. Lynch VJ, Leclerc RD, May G, Wagner GP. Transposon-mediated rewiring of gene  
597 regulatory networks contributed to the evolution of pregnancy in mammals. *Nat*  
598 *Genet.* 2011;43:1154–9.
- 599 22. Lynch VJ, Nnamani MC, Kapusta A, Brayer K, Plaza SL, Mazur EC, Emera D,  
600 Sheikh SZ, Grützner F, Bauersachs S, et al. Ancient transposable elements  
601 transformed the uterine regulatory landscape and transcriptome during the evolution  
602 of mammalian pregnancy. *Cell Rep.* 2015;10:551–61.
- 603 23. Schmidt D, Schwalie PC, Wilson MD, Ballester B, Gonçalves Â, Kutter C, Brown  
604 GD, Marshall A, Flicek P, Odom DT. Waves of retrotransposon expansion remodel  
605 genome organization and CTCF binding in multiple mammalian lineages. *Cell.*  
606 2012;148:335–48.
- 607 24. Chuong EB, Rumi MAK, Soares MJ, Baker JC. Endogenous retroviruses function as  
608 species-specific enhancer elements in the placenta. *Nat Genet.* 2013;45:325–9.
- 609 25. Chuong EB, Elde NC, Feschotte C. Regulatory evolution of innate immunity through  
610 co-option of endogenous retroviruses. *Science.* 2016;351:1083–7.
- 611 26. Jacques PE, Jeyakani J, Bourque G. 2013. The majority of primate-specific regulatory  
612 sequences are derived from transposable elements. *PLoS Genet* 9: e1003504.
- 613 27. Xie M, Hong C, Zhang B, Lowdon RF, Xing X, Li D, Zhou X, Lee HJ, Maire CL,  
614 Ligon KL, et al. DNA hypomethylation within specific transposable element families  
615 associates with tissue-specific enhancer landscape. *Nat Genet.* 2013;45:836–41.
- 616 28. del Rosario RCH, Rayan NA, Prabhakar S. Noncoding origins of anthropoid traits and  
617 a new null model of transposon functionalization. *Genome Res.* 2014;24:1469–84.
- 618 29. Sundaram V, Cheng Y, Ma Z, Li D, Xing X, Edge P, Snyder MP, Wang T.  
619 Widespread contribution of transposable elements to the innovation of gene  
620 regulatory networks. *Genome Res.* 2014;24:1963–76.
- 621 30. Pavlicev M, Hiratsuka K, Swaggart KA, Dunn C, and Muglia L Detecting  
622 Endogenous Retrovirus-Driven Tissue-Specific Gene Transcription. *Genome Biol*  
623 *Evol.* 2015;7(4):1082–97
- 624 31. Du J, Leung A, Trac C, Lee M, Parks BW, Lusk AJ, Natarajan R, Schones DE.  
625 Chromatin variation associated with liver metabolism is mediated by transposable  
626 elements. *Epigenetics Chromatin.* 2016;9:28.
- 627 32. Rayan NA, Del Rosario RCH, Prabhakar S. Massive contribution of transposable  
628 elements to mammalian regulatory sequences. *Semin Cell Dev Biol.* 2016;57:51–6.
- 629 33. Trizzino M, Park S, Holsbach-Beltrame M, Aracena K, Mika K, Caliskan M, Perry  
630 GH, Lynch V, Brown CD. Transposable elements are the primary source in the  
631 primate gene regulation. *Genome Res.* 2017;27:1623–33.



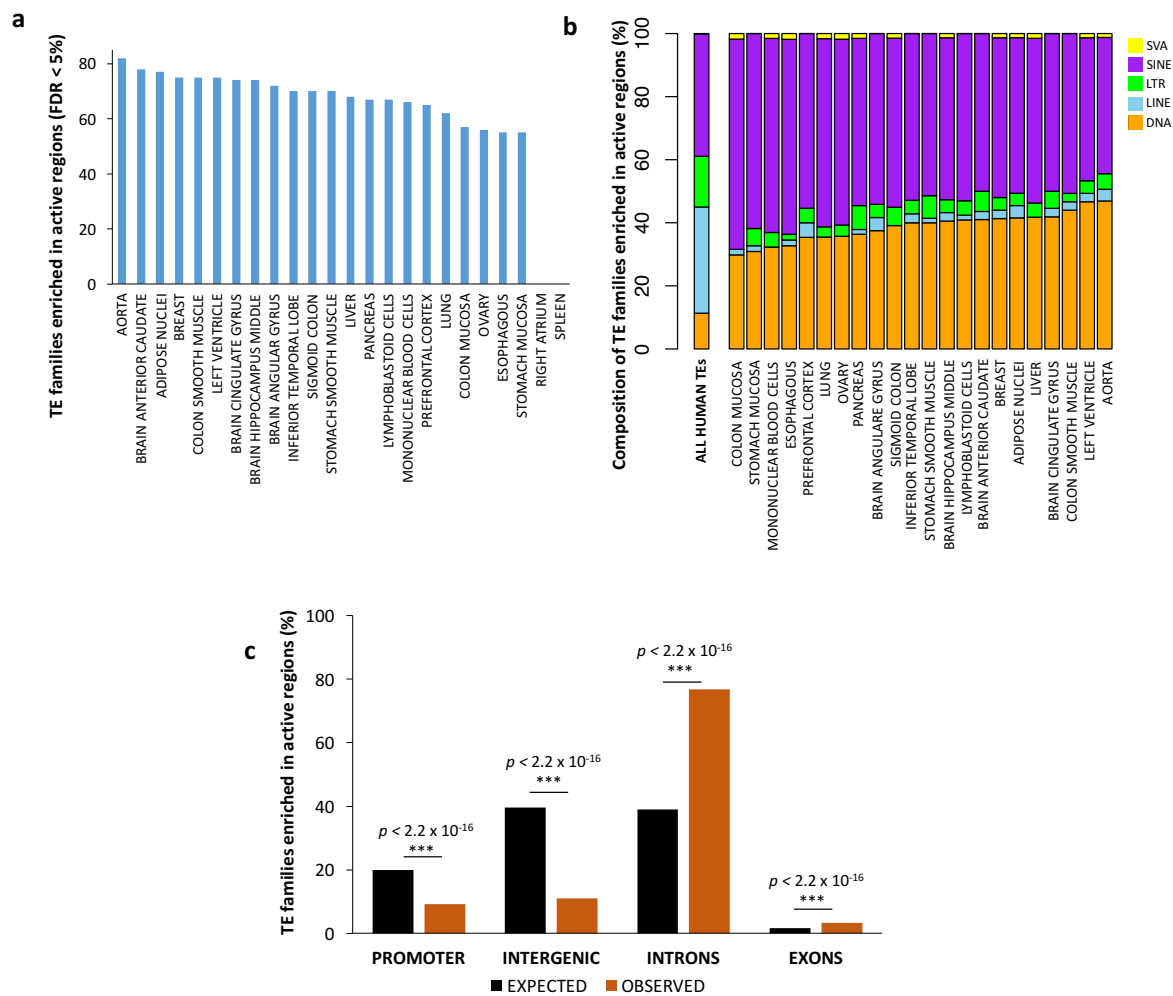
- 632 34. Macfarlan TS, et al. Embryonic stem cell potency fluctuates with endogenous  
633 retrovirus activity. *Nature*. 2012;487:57–63.
- 634 35. Simonti CN, Pavlicev M, Capra JA. Transposable Element Exaptation into  
635 Regulatory Regions is Rare, Influenced by Evolutionary Age, and Subject to  
636 Pleiotropic Constraints. *Mol Biol Evol*. 2017;34(11):2856–69.
- 637 36. Ward M, Zhao S, Luo K, Pavlovic B, Karimi MM, Stephens M, Gilad Y. Silencing of  
638 transposable elements may not be a major driver of regulatory evolution in primate  
639 induced pluripotent stem cells. *eLife*. 2018
- 640 37. Roadmap Epigenomics Mapping Consortium. Integrative analysis of 111 reference  
641 human epigenomes. *Nature*. 2015;518:317–30.
- 642 38. GTEx Consortium. Genetic effects on gene expression across human tissues. *Nature*.  
643 2017;550:204–13.
- 644 39. Kapusta A, Kronenberg Z, Lynch VJ, Zhuo X, Ramsay L, Bourque G, Yandell M,  
645 Feschotte C. Transposable elements are major contributors to the origin,  
646 diversification, and regulation of vertebrate long noncoding RNAs. *PLoS Genet*.  
647 2013;9:e1003470.
- 648 40. Klaver B, Berkhout B. Comparison of 5' and 3' long terminal repeat promoter function  
649 in human immunodeficiency virus. *J Virol*. 1994;68(6):3830–40.
- 650 41. Lavie L, Esther Maldener E, Brook Brouha B, Meese EU, Mayer J. The human L1  
651 promoter: Variable transcription initiation sites and a major impact of upstream  
652 flanking sequence on promoter activity. *Genome Res*. 2004;14:2253–60.
- 653 42. Walter M, Teissandier A, Pérez-Palacios R, Bouchis D. 2016. An epigenetic switch  
654 ensures transposon repression upon dynamic loss of DNA methylation in embryonic  
655 stem cells. *Elife*. 2016;5:e11418.
- 656 43. Daussy C, et al. T-bet and Eomes instruct the development of two distinct natural  
657 killer cell lineages in the liver and in the bone marrow. *J Exp Med*. 2014;3:563–77.
- 658 44. Gao F, et al. Integrated analyses of DNA methylation and hydroxymethylation reveal  
659 tumor suppressive roles of ECM1, ATF5, and EOMES in human hepatocellular  
660 carcinoma. *Genome Biol*. 2014;15:533–46.
- 661 45. Guo P, Dong X-Y, Zhao KW, Sun X, Li Q, Dong J-T. Estrogen-induced interaction  
662 between KLF5 and estrogen receptor (ER) suppresses the function of ER in ER-  
663 positive breast cancer cells. *Int J Cancer*. 2010;126(1):81–9.
- 664 46. Chen C, Bhalala HV, Qiao H, Dong JT. A possible tumor suppressor role of the KLF5  
665 transcription factor in human breast cancer. *Oncogene*. 2002;21:6567–6572.
- 666 47. Nagaoka K, Fujii K, Zhang H, Usuda K, Watanabe G, Ivshina M, Richter JD. CPEB1  
667 mediates epithelial-to-mesenchyme transition and breast cancer metastasis. *Oncogene*.  
668 2016;35:2893–901.
- 669 48. The ENCODE Project Consortium. An integrated encyclopedia of DNA elements in  
670 the human genome. *Nature*. 2012;489:57–74.
- 671 49. Furuyama K, et al. 2010. Continuous cell supply from a Sox9-expressing progenitor  
672 zone in adult liver, exocrine pancreas and intestine. *Nature Genetics*. 2010;43(1):35–  
673 42.



- 674 50. Cattoretti G, Angelin-Duclos C, Shaknovich R, Zhou H, Wang D, Alobeid B.  
675 PRDM1/Blimp-1 is expressed in human B-lymphocytes committed to the plasma cell  
676 lineage. *J Pathol.* 2005;206:76–86.
- 677 51. Cohen CJ, Lock WM, Mager DL. Endogenous retroviral LTRs as promoters for  
678 human genes: a critical assessment. *Gene.* 2009;448:105–14.
- 679 52. Janoušek V, Laukaitis CM, Yanchukov A, Karn R. The role of retrotransposons in  
680 gene family expansions in the human and mouse genomes. *Genome Biol Evol.*  
681 2016;8:2632–50.
- 682 53. Saykally JN, Dogan S, Cleary MP, Sanders MM. The ZEB1 Transcription Factor Is a  
683 Novel Repressor of Adiposity in Female Mice. *PlosONE.* 2009;4(12):e8460.
- 684 54. Gubelmann C, et al. Identification of the transcription factor ZEB1 as a central  
685 component of the adipogenic gene regulatory network. *eLIFE.* 2014;3:e03346.
- 686 55. Leow SC, et al. The transcription factor SOX6 contributes to the developmental  
687 origins of obesity by promoting adipogenesis. *Development.* 2016;143:950-61.
- 688 56. Alexandrov IM et al. 2012. Cytoplasmic Polyadenylation Element Binding Protein  
689 Deficiency Stimulates PTEN and Stat3 mRNA Translation and Induces Hepatic  
690 Insulin Resistance. *Plos Genet.* 2012;8(1):e1002457.
- 691 57. He G, Karin M. NF- $\kappa$ B and STAT3 – key players in liver in ammation and cancer.  
692 *Cell Res.* 2011;21:159-68.
- 693 58. Kelley D, Rinn J. Transposable elements reveal a stem cell-specific class of long  
694 noncoding RNAs. 2012;13(11):R107.
- 695 59. Beck, CM et al. LINE-1 Retrotransposition Activity in Human Genomes. *Cell.*  
696 2010;141:1159–70.
- 697 60. Muotri AR, Chu VT, Marchetto MC, Deng W, Moran JV, Gage FH. Somatic  
698 mosaicism in neuronal precursor cells mediated by L1 retrotransposition. *Nature.*  
699 2005;435(7044):903–10.
- 700 61. Coufal NG, Garcia-Perez JL, Peng GE, Yeo GW, Mu Y, Lovci MT, Morell M,  
701 O'Shea KS, Moran JV, Gage FH. L1 retrotransposition in human neural progenitor  
702 cells. *Nature.* 2009;460(7259):1127–31.
- 703 62. Upton KR, et al. Ubiquitous L1 mosaicism in hippocampal neurons. *Cell.*  
704 2017;161:228–39.
- 705 63. Sur D, et al. Detection of the LINE-1 retrotransposon RNA-binding protein ORF1p in  
706 different anatomical regions of the human brain. *Mobile DNA.* 2017;8:17.
- 707 64. Savage AL, et al. An evaluation of a SVA retrotransposon in the FUS promoter as a  
708 transcriptional regulator and its association to ALS. *Plos One.* 2014;9(6):e90833.
- 709 65. Smit A, Hubley R, Green P. RepeatMasker Open 4.0. 2013–2015. [http://](http://www.repeatmasker.org)  
710 [www.repeatmasker.org](http://www.repeatmasker.org). Benjamini Y, Hochberg Y. Controlling the false discovery  
711 rate: a practical and powerful approach to multiple testing. *J R Stat Soc B.*  
712 1995;57:289–300.
- 713 66. Quinlan AR, Hall IM. BEDTools: a flexible suite of utilities for comparing genomic  
714 features. *Bioinformatics.* 2010;26:841–2.
- 715 67. Benjamini Y, Hochberg Y. Controlling the false discovery rate: a prac- tical and  
716 powerful approach to multiple testing. *J R Stat Soc B.* 1995;57:289–300.

- 717 68. Bailey TL, et al. MEME SUITE: tools for motif discovery and searching. *Nucleic*  
718 *Acids Res.* 2009;37:W202–08
- 719 69. R Core Team. R: a language and environment for statistical computing. R Foundation  
720 for Statistical Computing, Vienna, Austria. 2016. <https://www.R-project.org/>.
- 721 70. Wickham H. *ggplot2: elegant graphics for data analysis*. 2009. Springer-Verlag, New  
722 York.
- 723
- 724
- 725
- 726
- 727
- 728
- 729
- 730
- 731
- 732
- 733
- 734
- 735
- 736
- 737
- 738
- 739
- 740
- 741
- 742
- 743
- 744
- 745
- 746

747



748

749 **Figure 1 - Transposable elements are enriched in active genomic regions. (A)**

750 The plot displays the numbers of enriched TE families in the active genomic regions

751 for each tissue (FDR < 5%). The distribution suggests a tissue-specific pattern. (B)

752 Stacked-bar charts show TE class composition for the TE families enriched in active

753 regions (FDR < 5%). SINE and DNA transposons are the dominant TEs enriched in

754 active regions. (C) The TEs enriched in active regions are depleted from promoters

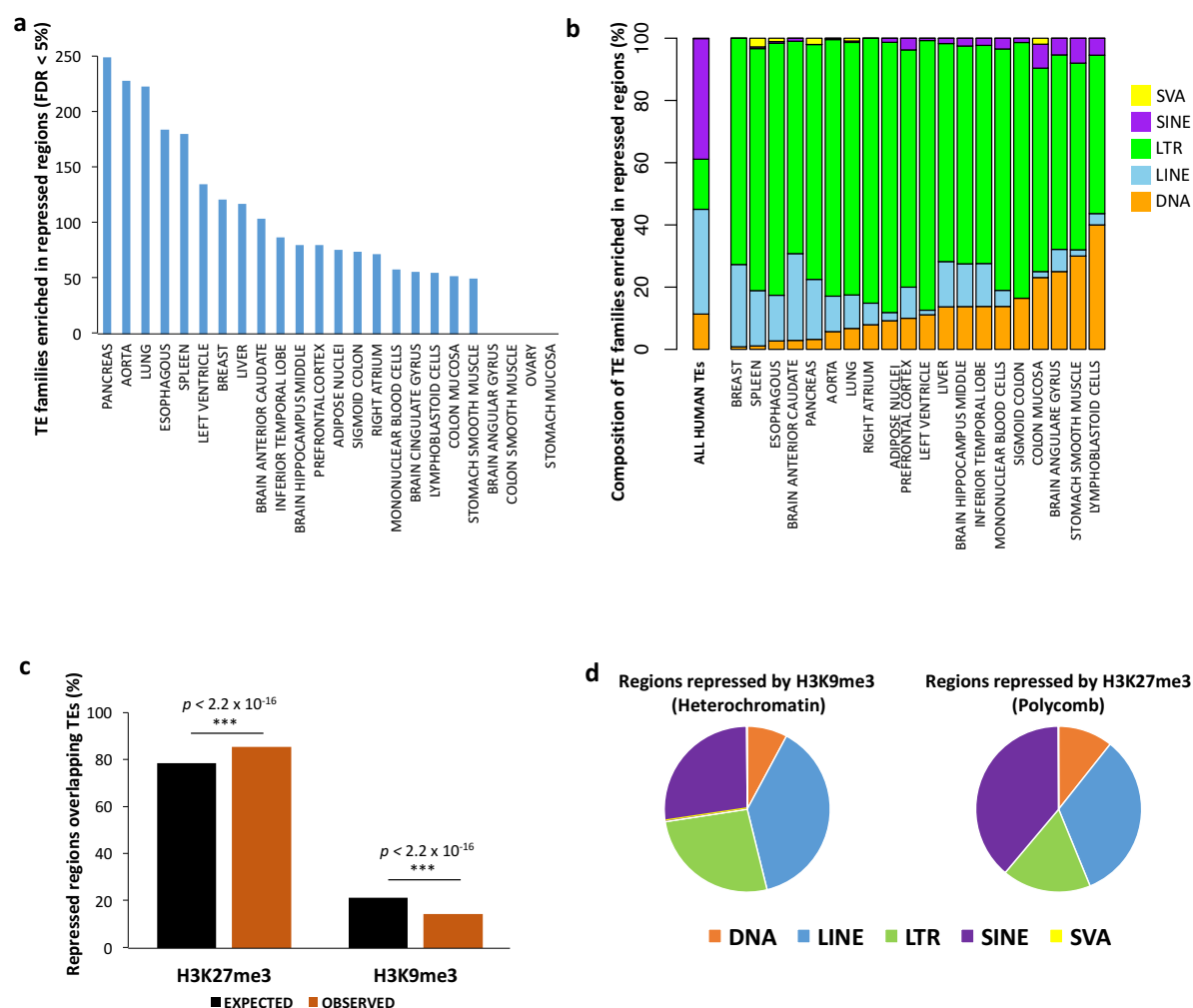
755 and intergenic regions, while they are significantly enriched in intronic regions.

756

757

758

759



760

761

762 **Figure 2 - Transposable elements are enriched in repressed genomic regions.**

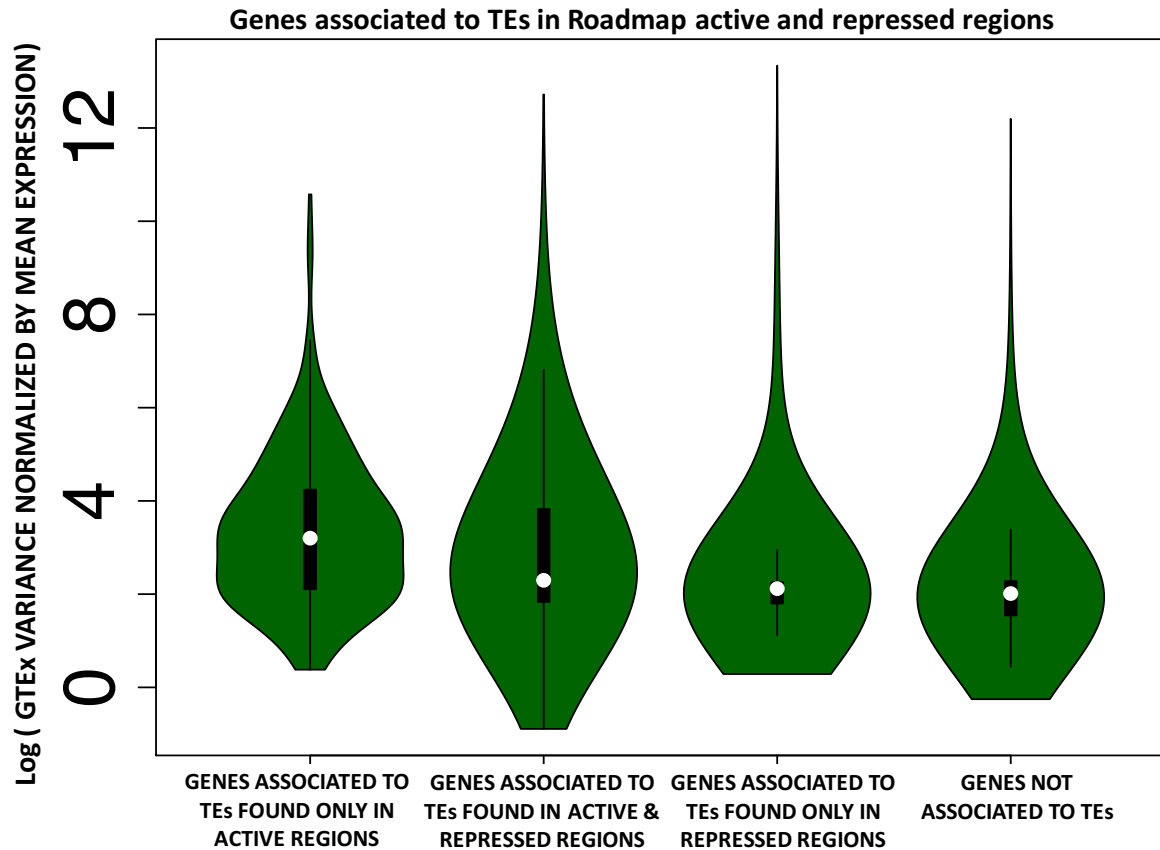
763 (A) The plot displays the numbers of enriched TE families in the repressed genomic  
 764 regions for each tissue (FDR < 5%). The distribution suggests a tissue-specific  
 765 pattern. (B) Stacked-chart plot shows class composition for the TE families enriched  
 766 in repressed regions (FDR < 5%). (C) Across tissues, the repressed TEs overlap  
 767 H3K27me3 more than expected by chance, while H3K9me3 is underrepresented.  
 768 (D) Pie-charts show class composition for the TEs overlapping H3K27me3 and  
 769 H3K9me3.

770

771

772

773



774

775

776 **Figure 3 - Genes with higher expression variance are more tolerant towards TE**  
777 **expression.** Human genes were split into four categories: 1) Genes associated with  
778 TEs that are only found in active regions across tissues; 2) Genes associated with  
779 TEs that are found in active or repressed regions in a tissue-specific fashion; 3)  
780 Genes associated with TEs that are only found in repressed regions; 4) Genes never  
781 associated with TE insertions. The violin plots display the distribution of the GTEx  
782 gene expression variance, normalized by mean expression, for each of the four  
783 categories.

784

785

786

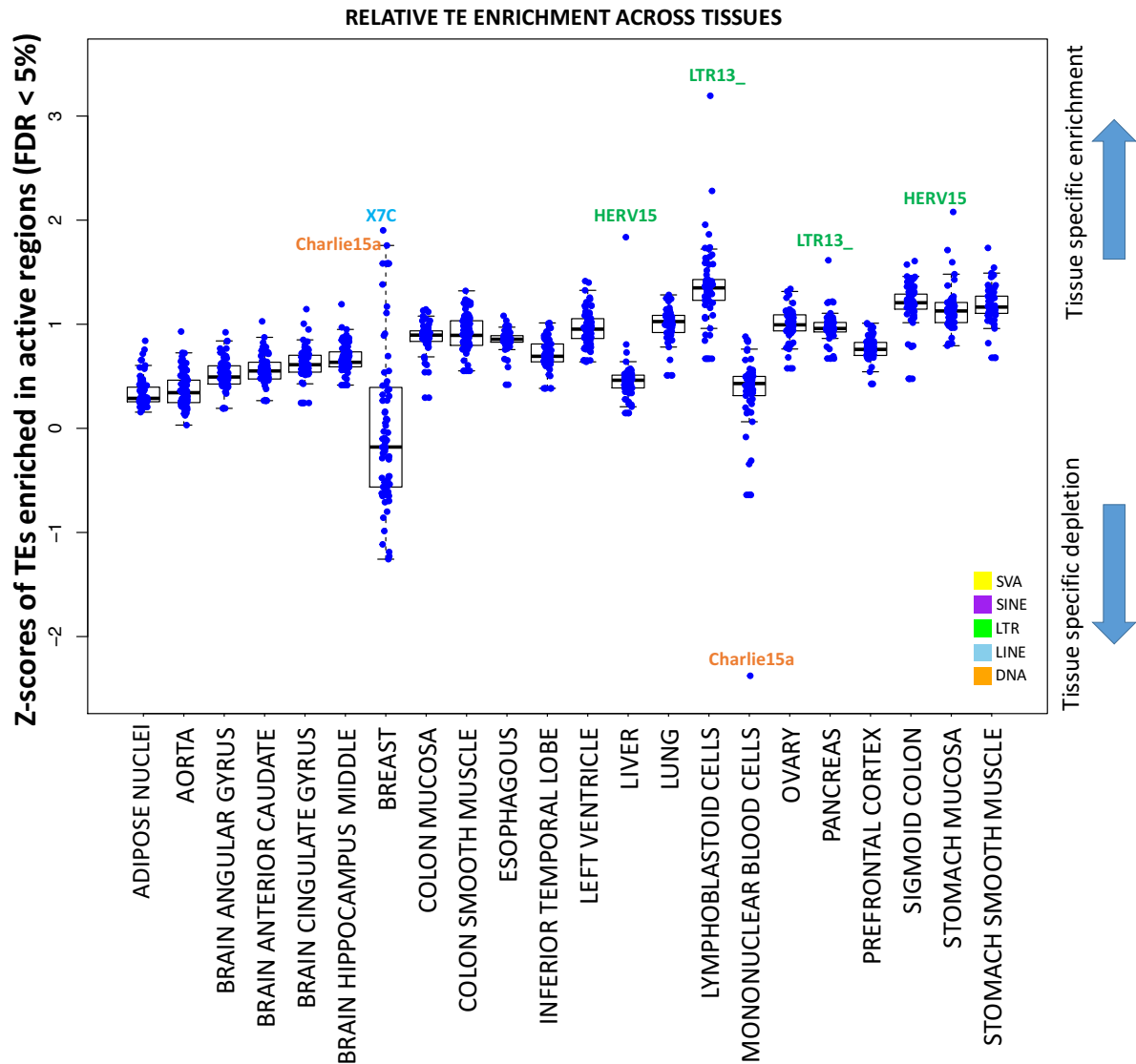
787

788

789

790

791



792

793

794 **Figure 4 - Transposable elements have tissue-specific enrichment in active**  
 795 **regions.** The plot displays the distribution of the effect sizes (Z-scores from  
 796 permutation test, see methods) for each TE enriched in active regions (FDR < 5%),  
 797 in each tissue. The higher the Z-score, the more tissue-specific is the enrichment.  
 798

798

799

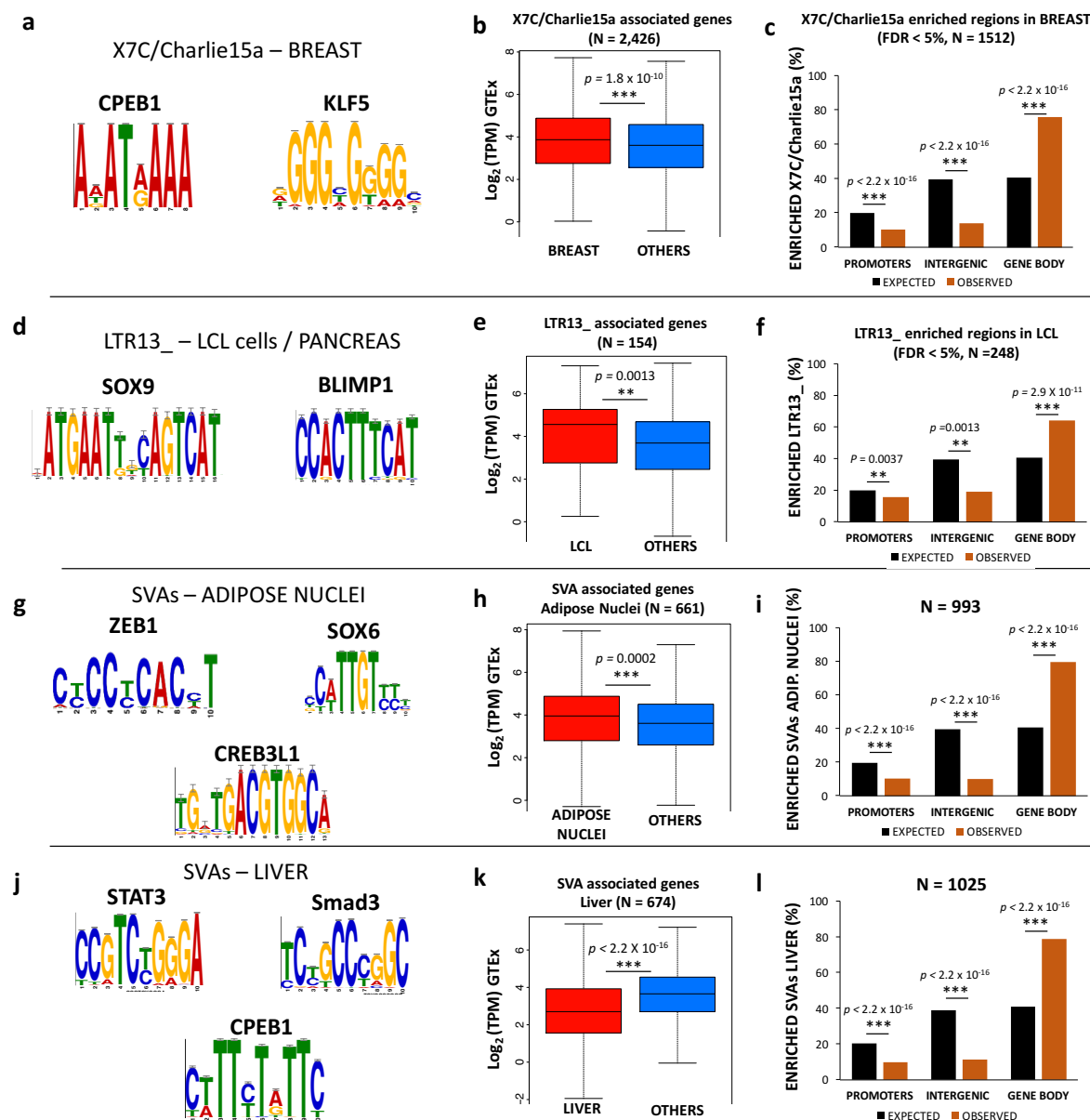
800

801

802

803

804



805

806 **Figure 5 - Tissue-specific TEs are enriched for TF binding sites, are mostly**  
 807 **intronic, and affect gene expression.** (a) Motifs enriched in the regions  
 808 overlapping X7C and and Charlie15a TEs in the breast. (b) Boxplot comparing mean  
 809 expression for the genes associated to X7C and and Charlie15a in the breast vs all  
 810 the other tissues. (c) Genomic distribution of the regions overlapping X7C and and  
 811 Charlie15a TEs in the breast. (d) Motifs enriched in the regions overlapping LTR13\_  
 812 TEs in pancreas and LCL cells. (e) Boxplot comparing mean expression for the  
 813 genes associated to LTR13\_ in the LCLs vs all the other tissues. (f) Genomic  
 814 distribution of the regions overlapping LTR13\_ in the LCLs. (g) Motifs enriched in the  
 815 regions overlapping SVAs in the adipose nuclei. (h) Boxplot comparing mean  
 816 expression for the genes associated to SVAs in the adipose nuclei vs all the other  
 817 tissues. (i) Genomic distribution of the regions overlapping SVAs in the adipose  
 818 nuclei. (j) Motifs enriched in the regions overlapping SVAs in the liver. (k) Boxplot  
 819 comparing mean expression for the genes associated to SVAs in the liver vs all the  
 820 other tissues. (l) Genomic distribution of the regions overlapping SVAs in the liver.  
 821